π-mode solitons in photonic Floquet lattices

Hua Zhong (钟华),[1] Yaroslav V. Kartashov [ORCID],[2] Yongdong Li (李永东),[1] and Yiqi Zhang (张贻齐) [ORCID][1,*]

[1]*Key Laboratory for Physical Electronics and Devices of the Ministry of Education & Shaanxi Key Lab of Information Photonic Technique, School of Electronic and Information Engineering, Xi'an Jiaotong University, Xi'an 710049, China*
[2]*Institute of Spectroscopy, Russian Academy of Sciences, Troitsk, Moscow 108840, Russia*

We report on the existence and stability of π-mode solitons in both one-dimensional (1D) and two-dimensional (2D) nonlinear Su-Schrieffer-Heeger (SSH) arrays with periodic longitudinal modulation that mimics temporal periodic driving in Floquet systems. The SSH array is a paradigmatic example of the topological insulator, where edge states appear for the proper ratio of the intra- and intercell couplings. When the SSH array is additionally periodically driven due to longitudinal oscillations of waveguide centers, so that for half of the driving cycle it is in trivial phase, while on other half it is in topological phase, a new type of anomalous topological π-mode emerges at the edges of the driven lattice. We consider π-mode solitons with propagation constants in the gap of this equivalent Floquet system bifurcating under the action of nonlinearity from anomalous linear π-mode states. In the 1D case such periodically oscillating solitons become more robust with an increase of the amplitude of oscillations of waveguide positions and survive over hundreds of longitudinal lattice periods. We also found that they can be very robust in the 2D equivalent Floquet SSH arrays. Furthermore, we show that π-mode solitons can be directly excited by Gaussian beams launched into the array at the proper distance. Our results suggest a framework for experimental observation of the π-mode solitons, including in higher-order topological Floquet systems.

The concept of photonic topological insulators [1–11] that substantially develops the ideas about the existence of topological edge states formulated in solid-state physics [12,13] has received increasing attention in the past decade. Various schemes for observation of photonic topological insulators have been proposed [14–26]. The first realization of a topological Chern insulator at optical frequencies—a photonic Floquet topological insulator—was demonstrated using helical waveguides arranged into a honeycomb array [20], where the gauge field resulting from waveguide rotation breaks the effective time-reversal symmetry of the system. The Floquet mechanism arising from periodic driving in the temporal domain [27] can be mimicked in such systems by periodic modulation of the waveguide array along the propagation direction [28–31], which has been used for demonstration of anomalous topological phase transitions [32,33], perfect subwavelength self-imaging [34], edge-state coupling [35,36], and tunneling inhibition [37].

Several special designs are of particular interest that allow one to generate so-called anomalous Floquet topological π-modes which can be depicted by the π-gap invariant [38–42]. Such localized but strongly oscillating states can be observed, for example, when periodic modulation in the evolution variable is introduced into the Su-Schrieffer-Heeger (SSH) array to affect inter- and intracell couplings [43]. Until now, anomalous Floquet topological π-modes have been experimentally observed in the ultrathin metallic arrays of coupled corrugated

waveguides [44], in non-Hermitian and conservative waveguide arrays [45,46], and in evanescently coupled plasmonic structures [47]. However, all such π-mode states have been studied so far only in the linear regime. Recently, linear π/2-modes were reported in an acoustic Floquet system [48].

On the other hand, nonlinearity may be crucial for manipulation, control, and sometimes even for the existence of the topological edge states [49]. A plethora of intriguing phenomena appearing due to nonlinearity have been reported in topological systems, including modulational instability [50] and bistability of the unidirectional edge states [51], topological transitions [52–54], formation of topological solitons [55–62], and breakdown of topological transport [63–65]. The question of whether π-mode states can exist in nonlinear Floquet systems remains unaddressed not only in one-dimensional (1D) systems but especially in two-dimensional (2D) systems. In the presence of nonlinearity it is unclear whether such self-sustained states can avoid radiation and, in 2D cases, collapse. Even though Floquet solitons have been reported here and there [56,66], π-mode solitons are still open for exploration.

In this Letter, we report on the 1D and 2D π-mode solitons. We carry out our analysis using a continuous model, accounting for the exact shape of the longitudinally modulated waveguide array. Using a self-consistent iterative procedure [55], we find solitons showing exactly periodic evolution on one driving period and determine the range of amplitudes, where such solitons show robust propagation over multiple longitudinal periods when they are perturbed. We show that nonlinearity allows one to control the location of
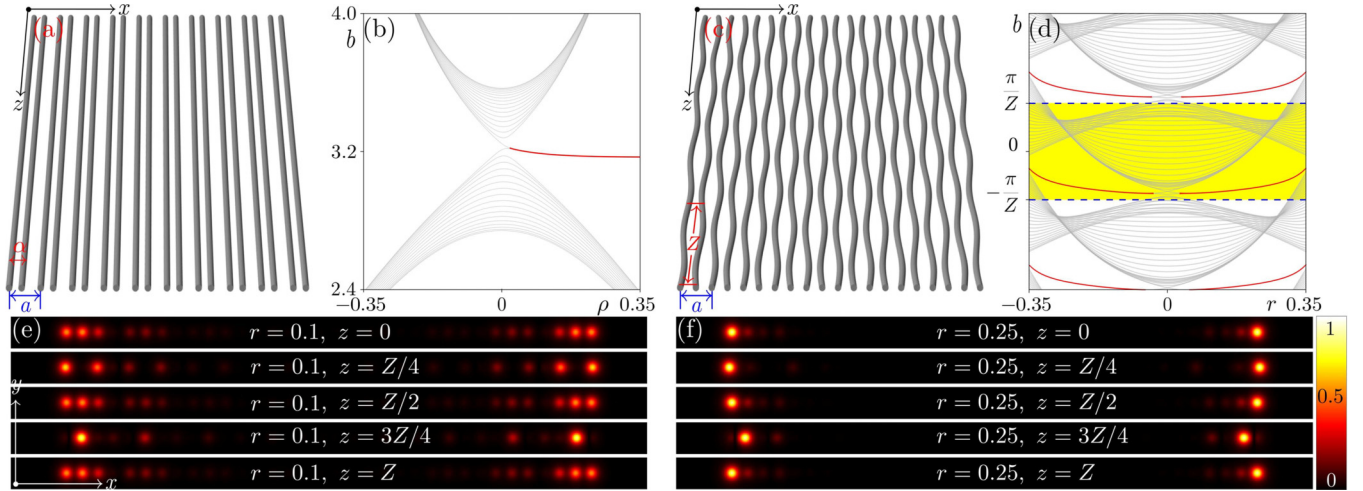
*zhangyiqi@xjtu.edu.cn

L021502-1

FIG. 1. (a) Straight 1D SSH waveguide array. (b) Spectrum of static array versus $\rho = \alpha - a/2$. The array depicted in panel (a) corresponds to $\alpha = 0.4a$, i.e., $\rho = -0.1a$. (c) Dynamic 1D SSH array, where waveguides in each unit cell oscillate out of phase. (d) Floquet spectrum of the array from panel (c) for various r values. The π-mode is highlighted by the red color. The yellow region between two dashed lines indicates the first longitudinal Brillouin zone. π-modes at different distances for $r = 0.1$ (e) and $r = 0.25$ (f). All modes are shown within the windows $-32 \leqslant x \leqslant 32$ and $-1.6 \leqslant y \leqslant 1.6$.

quasienergies of such solitons within the gap and strongly affects their spatial localization. Moreover, we found that such solitons can exist in both focusing and defocusing materials and that they are robust and survive even in the presence of defects in the array.

We consider the propagation of a light beam in a modulated waveguide array described by the dimensionless Schrödinger-like paraxial wave equation with cubic nonlinearity:

$$i\frac{\partial \psi}{\partial z} = -\frac{1}{2}\left(\frac{\partial^2}{\partial x^2} + \frac{\partial^2}{\partial y^2}\right)\psi - \mathcal{R}(x, y, z)\psi - \sigma|\psi|^2\psi. \quad (1)$$

Here, ψ is the light field amplitude, x and y are the normalized transverse coordinates, z is the propagation distance that plays in Eq. (1) the same role as time in the Schrödinger equation describing a quantum particle in a potential, the function $\mathcal{R}(x, y, z)$ describes the array with longitudinal modulation, and $\sigma = 1$ ($\sigma = -1$) corresponds to the focusing (defocusing) nonlinearity. In the 1D case, the function describing the array structure can be written as $\mathcal{R}(x, y, z) = p\sum_m e^{-(x_{1m}^2 + y^2)/d^2} + e^{-(x_{2m}^2 + y^2)/d^2}$, where $x_{1m} = x_m - a/4 - r\sin(\omega z)$ and $x_{2m} = x_m + a/4 + r\sin(\omega z)$ with $\omega = 2\pi/Z$, Z is the modulation period, $x_m = x + ma$ with m being an integer, r is the amplitude of waveguide oscillations, a is the unit cell size (separation between two next-nearest-neighbor channels), and d is the waveguide width. The separation between two guides in the unit cell (intracell separation) varies dynamically and is given by $a/2 - 2r\sin(\omega z)$.

We use parameters $a = 3.2$ ($\sim 32\,\mu m$), $d = 0.5$ ($\sim 5\,\mu m$), $Z = 10$ (~ 1.1 cm), and $p = 10$ ($\sim 1 \times 10^{-3}$), representative of femtosecond-laser-written waveguide arrays and experiments at $\lambda = 800$ nm [61,67,68]. In the 2D array (Fig. 4) four waveguides in the unit cell are allowed to oscillate along the diagonal of the unit cell [69]. Note that the system considered here is equivalent to the Floquet system, since driving in time is mimicked here by the periodic modulation along the propagation direction z.

Neglecting the nonlinear term in Eq. (1) and introducing the ansatz $\psi = u(x, y, z)e^{ibz}$, with b being a quasipropagation constant and $u(x, y, z)$ being a Z-periodic complex field, we obtain the problem $bu = (\partial_x^2 + \partial_y^2)u/2 + \mathcal{R}u + i\partial_z u$, which can be solved numerically using propagation and the projection method adopted in Refs. [59,70,71]. If the array represents the standard "static" 1D SSH structure, as shown in Fig. 1(a), where α is the adjustable intracell separation, it supports edge states only in the topological regime with $\alpha > a/2$, as indicated by the red line in the spectrum displayed in Fig. 1(b). To make sure that the forbidden gap is fully developed, here we use a large array with 34 waveguides. If, however, the array is periodically modulated with a period Z, as shown in Fig. 1(c), it spends half of the driving cycle in the topological phase (when intercell coupling is stronger than the intracell one and edge states should be present) and half in the trivial one (where edge states would not exist in the static case). Still, regardless of the sign of r, which in our case determines the phase of waveguide oscillations, a modulated array supports topological anomalous π-mode edge states for a broad range of $|r|$ values, as indicated by the red lines in the quasipropagation constant spectrum in Fig. 1(d) [72], where the spectrum is periodic in b with the first Brillouin zone (BZ) illustrated by the yellow region between the two dashed lines. Anomalous π-modes exhibit strong shape variations upon propagation, but remain exactly Z-periodic. This is seen from Figs. 1(e) and 1(f), where we display $|\psi|$ distributions at selected distances for $r = 0.1$ and $r = 0.25$, respectively. Since the mode at $r = 0.1$ is closer to the bulk band, it is less localized than the mode at $r = 0.25$. Although the field modulus distributions are identical at distances $z = Z/2$ and $z = Z$, the profiles at $z = Z/4$ and $z = 3Z/4$ are different, indicating the fact that the full period is Z.

Next we consider π-mode solitons that bifurcate from linear anomalous π-modes. Remarkably, such solitons exist for both focusing and defocusing nonlinearities [72]. We display
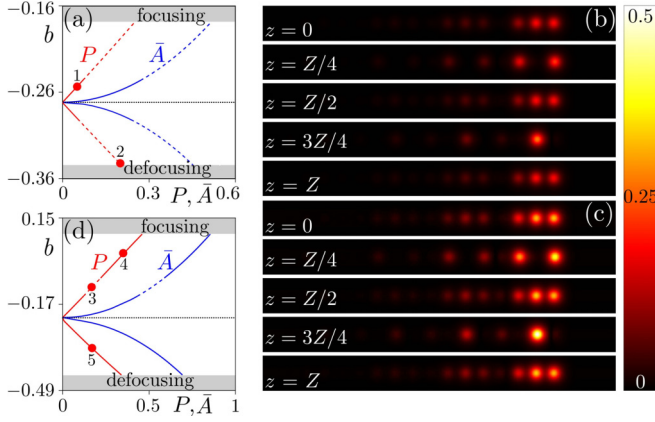
FIG. 2. (a) Quasipropagation constant b versus averaged peak amplitude $\bar{A}$ and power P showing the π-mode soliton family at $r = 0.1$. Dashed lines represent unstable solitons, solid lines represent stable ones, and the shaded regions are bulk bands. $|\psi|$ distributions at different distances in π-mode solitons with $P = 0.05$ in the focusing medium (b) and with $P = 0.2$ in the defocusing medium (c), corresponding to dots 1 and 2 in panel (a), respectively. Profiles are shown within the $0 \leqslant x \leqslant 32$ and $-1.6 \leqslant y \leqslant 1.6$ windows. (d) π-mode soliton family at $r = 0.25$.

FIG. 3. Panels (a) and (b) show propagation dynamics in z (cross section at $y = 0$) of π-mode solitons corresponding to dots 3 (unstable state with $P = 0.17$) and 4 (stable state with $P = 0.35$) in Fig. 2(d), respectively, while panel (c) shows corresponding peak amplitudes of the states marked with dots 3–5. (d)–(g) Propagation dynamics in z for Gaussian inputs with different powers. Here $r = 0.25$.

the relation between the quasipropagation constant b and the power P of the π-mode soliton and between b and the averaged peak amplitude $\bar{A} = \int_0^Z A dz/Z$, where $A = |\psi|_{\max}$, in Fig. 2(a) at $r = 0.1$. One can see that the power P of the π-mode soliton exhibits a linear behavior with b which departs from the value corresponding to the linear π-mode (where $\bar{A}, P \to 0$), while the averaged amplitude shows nonlinear behavior. Thus, nonlinearity allows one to tune the localization of states by changing the location of b in the gap. At sufficiently high powers, when b is close to the bulk band, the soliton couples with the bulk modes and acquires long tails for both focusing and defocusing nonlinearities [this tendency is clear in Fig. 2(c) corresponding to dot 2 in Fig. 2(a)].

The stability of π-mode solitons was examined by adding a small-scale noise with an amplitude up to $0.1A$ into input states and propagating them over a large distance, e.g., $z \sim 4000$. Stable and unstable families are shown in Fig. 2(a) by solid and dashed lines, respectively. At $r = 0.1$, solitons become unstable when their power exceeds $P \approx 0.07$. Examples of π-mode solitons in focusing ($P = 0.05$) and defocusing ($P = 0.2$) media are shown in Figs. 2(b) and 2(c), respectively. By increasing the amplitude of waveguide oscillations to $r = 0.25$, as shown in Fig. 2(d), we were able to substantially extend stability domains for π-mode solitons. Surprisingly, in the focusing case with the increase of P the π-mode soliton first becomes unstable within a small range of powers and then stabilizes again. For this r, the π-mode soliton is always stable in the defocusing medium. Propagation dynamics of unstable [dot 3 in Fig. 2(d)] and stable [dot 4 in Fig. 2(d)] solitons in the focusing medium are depicted in Figs. 3(a) and 3(b), respectively. In Fig. 3(c), peak amplitudes of the solitons in the focusing medium from Figs. 3(a) and 3(b) as well as of stable solitons in the defocusing medium [dot 5 in Fig. 2(d)] during propagation are exhibited. The unstable state radiates into the bulk upon
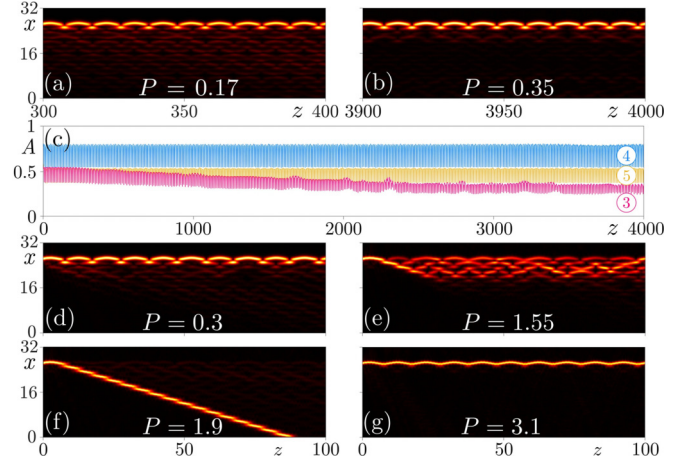
propagation with the radiation rate decreasing with z [see Fig. 3(a) and the magenta curve in Fig. 3(c)]. In contrast, stable π-mode solitons show persistent oscillations without any sign of radiation over very long distances [see blue and yellow curves in Fig. 3(c)]. Thus, nonlinearity not only allows one to control the localization of π-mode states but it may also cause spontaneous emission that shifts unstable states into stable domains. Importantly, we also found that the π-mode solitons presented here are robust and survive even in the presence of defects in the array [72].

To stress the experimental relevance of our findings, we show that π-mode solitons can be excited by injecting a single Gaussian beam into the edge waveguide. Different propagation scenarios were encountered depending on the power P of the input beam. At power levels not exceeding powers of π-mode solitons in the gap, we observe efficient soliton excitation after some reshaping (sometimes with weak radiation into the bulk) at the initial stages of propagation [Fig. 3(d)]. At somewhat larger powers nonlinearity leads to strong coupling with bulk modes and we observe the formation of irregularly oscillating moderately extended states in the vicinity of the edge [Fig. 3(e)]. When power increases even further, the excitation of traveling into the bulk well-localized soliton occurs [Fig. 3(f)]. For $r = 0.25$, this happens when $1.8 \leqslant P \leqslant 2.4$. Finally, the propagation dynamics in Fig. 3(g) corresponds to a very strong nonlinearity, when all light remains in the excited channel. This regime is reminiscent of excitation of high-power solitons from a semi-infinite gap in the static array.

We now consider π-mode solitons in a 2D SSH array. The schematic illustration of such a "static" array [73–75], where nontrivial topology can be introduced by changing intercell separation α between four waveguides in the unit cell, is shown in Fig. 4(a). Its static spectrum as a function of the parameter $\rho = \alpha - a/2$ is depicted in Fig. 4(b). The red line corresponds to corner states appearing at $\alpha > a/2$ (or $\rho > 0$).
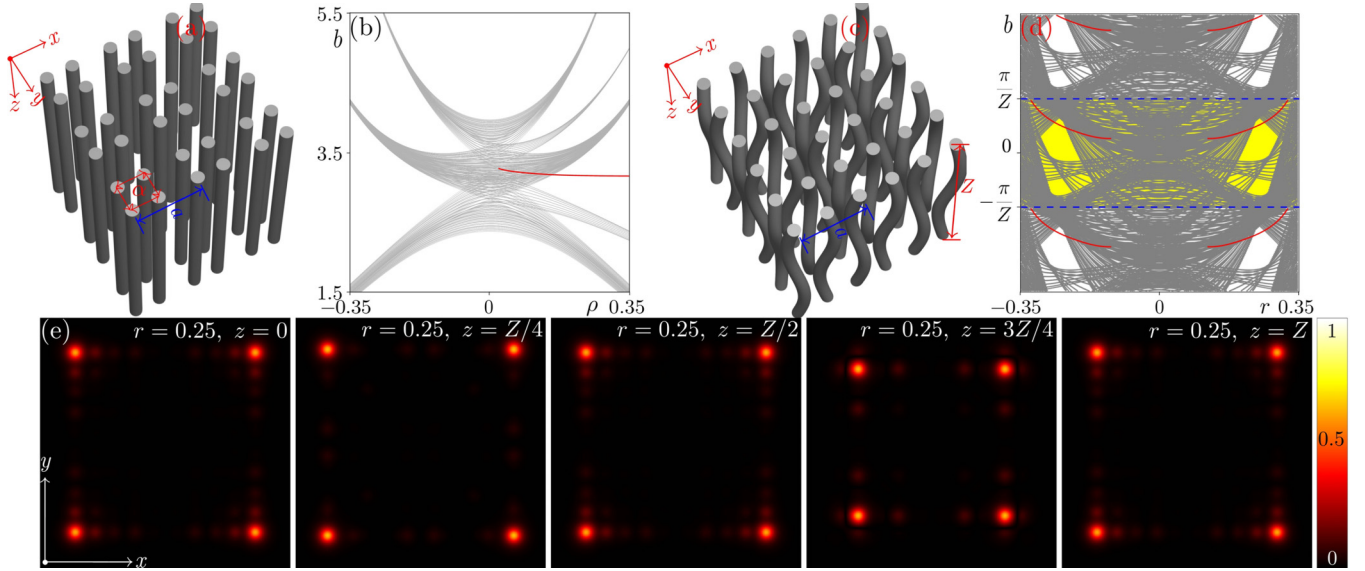
FIG. 4. Properties of linear π-mode states in 2D SSH arrays. Panels (a) and (b) show the static 2D SSH array and spectrum of its modes, respectively. Panels (c) and (d) show the modulated 2D SSH array and its quasipropagation constant spectrum, respectively. Mode profiles in panel (e) are shown within $-10 \leqslant x \leqslant 10$ and $-10 \leqslant y \leqslant 10$ windows for $r = 0.25$.

They may partially overlap with the bulk band at $\rho < 0.16$ as observed also in Ref. [62]. When this array is periodically driven, so that waveguide positions oscillate periodically along the diagonal of the unit cell, 2D linear π-modes emerge. The periodically driven structure that we consider in this Letter is schematically depicted in Fig. 4(c), while its linear quasipropagation constant spectrum is displayed in Fig. 4(d) as a function of the oscillation amplitude r. First the longitudinal BZ is highlighted by the yellow color; its boundaries are indicated by the dashed lines. Linear π-modes localized in the corners of this structure are shown by the red lines in the spectrum. Due to band folding [59,70,71] π-modes may overlap with bulk states, but there are also oscillation amplitudes r, when such states appear in the gap (this gap remains practically unchanged with increase of the array size).

In Fig. 4(e) we show the profile $|\psi|$ of the well-localized π-mode at different propagation distances for $r = 0.25$ that illustrates its exact Z-periodic behavior. Localization of the linear π-mode for $r = 0.1$ (not shown here) is substantially weaker. It should be stressed that array images in Figs. 4(a) and 4(c) schematically show only several unit cells of the structure, while the entire structure used for simulations contains 100 waveguides.

The families of 2D π-mode solitons in both focusing and defocusing media bifurcating from the linear π-mode state at $r = 0.25$, which is completely in the band gap [72], are displayed in Fig. 5(a). Despite considerable but periodic oscillations that such nonlinear 2D states undergo in the process of propagation, they remain stable for selected r values. Figure 5(b) displays two representative π-mode solitons at $z = 0$ that correspond to dots 1 and 2 in Fig. 5(a). Note the considerable shape transformation of the π-mode caused by the nonlinearity. For our parameters such nonlinear states, when perturbed by small-scale noise, show stable propagation for both signs of nonlinearity, as illustrated by the dependence of the peak amplitude A on the distance z in Fig. 5(c).

Summarizing, we have shown that periodically driven SSH arrays can support stable π-mode solitons in both 1D and 2D settings. Our results may be promising for observation of various nonlinear phenomena in Floquet higher-order topological insulators [76–78]. They may be also extended to various nonequilibrium Floquet systems [27], for example, for the design of lasers based on π-modes.
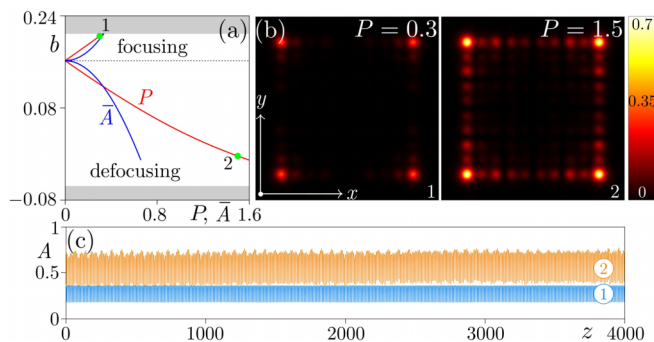

FIG. 5. (a) Family of 2D π-mode solitons and (b) examples of their profiles at $z = 0$ corresponding to dots in panel (a). Gray regions in panel (a) represent bulk bands. (c) Peak amplitude of the perturbed π-mode solitons corresponding to dots 1 and 2 in panel (a) versus z. In all cases $r = 0.25$.

[1] L. Lu, J. D. Joannopoulos, and M. Soljačić, Topological photonics, Nat. Photonics **8**, 821 (2014).

[2] T. Ozawa, H. M. Price, A. Amo, N. Goldman, M. Hafezi, L. Lu, M. C. Rechtsman, D. Schuster, J. Simon, O. Zilberberg, and I. Carusotto, Topological photonics, Rev. Mod. Phys. **91**, 015006 (2019).

[3] H. Price, Y. Chong, A. Khanikaev, H. Schomerus, L. J. Maczewsky, M. Kremer, M. Heinrich, A. Szameit, O. Zilberberg, Y. Yang, B. Zhang, A. Alù, R. Thomale, I. Carusotto, P. St-Jean, A. Amo, A. Dutt, L. Yuan, S. Fan, X. Yin *et al.*, Roadmap on topological photonics, J. Phys. Photonics **4**, 032501 (2022).

[4] Q. Yan, X. Hu, Y. Fu, C. Lu, C. Fan, Q. Liu, X. Feng, Q. Sun, and Q. Gong, Quantum topological photonics, Adv. Opt. Mater. **9**, 2001739 (2021).

[5] Y. Ota, K. Takata, T. Ozawa, A. Amo, Z. Jia, B. Kante, M. Notomi, Y. Arakawa, and S. Iwamoto, Active topological photonics, Nanophotonics **9**, 547 (2020).

[6] M. Kim, Z. Jacob, and J. Rho, Recent advances in 2D, 3D and higher-order topological photonics, Light: Sci. Appl. **9**, 130 (2020).

[7] M. Parto, Y. G. N. Liu, B. Bahari, M. Khajavikhan, and D. N. Christodoulides, Non-Hermitian and topological photonics: Optics at an exceptional point, Nanophotonics **10**, 403 (2021).

[8] H. Wang, S. K. Gupta, B. Xie, and M. Lu, Topological photonic crystals: A review, Front. Optoelectron. **13**, 50 (2020).

[9] H. Xue, Y. Yang, and B. Zhang, Topological valley photonics: Physics and device applications, Adv. Photonics Res. **2**, 2100013 (2021).

[10] G.-J. Tang, X.-T. He, F.-L. Shi, J.-W. Liu, X.-D. Chen, and J.-W. Dong, Topological photonic crystals: Physics, designs, and applications, Laser Photonics Rev. **16**, 2100300 (2022).

[11] Z. Lan, M. L. Chen, F. Gao, S. Zhang, and W. E. I. Sha, A brief review of topological photonics in one, two, and three dimensions, Rev. Phy. **9**, 100076 (2022).

[12] M. Z. Hasan and C. L. Kane, Colloquium: Topological insulators, Rev. Mod. Phys. **82**, 3045 (2010).

[13] X.-L. Qi and S.-C. Zhang, Topological insulators and superconductors, Rev. Mod. Phys. **83**, 1057 (2011).

[14] F. D. M. Haldane and S. Raghu, Possible Realization of Directional Optical Waveguides in Photonic Crystals with Broken Time-Reversal Symmetry, Phys. Rev. Lett. **100**, 013904 (2008).

[15] Z. Wang, Y. Chong, J. D. Joannopoulos, and M. Soljačić, Observation of unidirectional backscattering-immune topological electromagnetic states, Nature (London) **461**, 772 (2009).

[16] N. H. Lindner, G. Refael, and V. Galitski, Floquet topological insulator in semiconductor quantum wells, Nat. Phys. **7**, 490 (2011).

[17] M. Hafezi, E. A. Demler, M. D. Lukin, and J. M. Taylor, Robust optical delay lines with topological protection, Nat. Phys. **7**, 907 (2011).

[18] Y. Yang, Z. Gao, H. Xue, L. Zhang, M. He, Z. Yang, R. Singh, Y. Chong, B. Zhang, and H. Chen, Realization of a three-dimensional photonic topological insulator, Nature (London) **565**, 622 (2019).

[19] A. B. Khanikaev, S. H. Mousavi, W.-K. Tse, M. Kargarian, A. H. MacDonald, and G. Shvets, Photonic topological insulators, Nat. Mater. **12**, 233 (2013).

[20] M. C. Rechtsman, J. M. Zeuner, Y. Plotnik, Y. Lumer, D. Podolsky, F. Dreisow, S. Nolte, M. Segev, and A. Szameit, Photonic Floquet topological insulators, Nature (London) **496**, 196 (2013).

[21] M. Hafezi, S. Mittal, J. Fan, A. Migdall, and J. M. Taylor, Imaging topological edge states in silicon photonics, Nat. Photonics **7**, 1001 (2013).

[22] W.-J. Chen, S.-J. Jiang, X.-D. Chen, B. Zhu, L. Zhou, J.-W. Dong, and C. T. Chan, Experimental realization of photonic topological insulator in a uniaxial metacrystal waveguide, Nat. Commun. **5**, 5782 (2014).

[23] G. Q. Liang and Y. D. Chong, Optical Resonator Analog of a Two-Dimensional Topological Insulator, Phys. Rev. Lett. **110**, 203904 (2013).

[24] F. Gao, Z. Gao, X. Shi, Z. Yang, X. Lin, H. Xu, J. D. Joannopoulos, M. Soljačić, H. Chen, L. Lu, Y. Chong, and B. Zhang, Probing topological protection using a designer surface plasmon structure, Nat. Commun. **7**, 11619 (2016).

[25] L.-H. Wu and X. Hu, Scheme for Achieving a Topological Photonic Crystal by Using Dielectric Material, Phys. Rev. Lett. **114**, 223901 (2015).

[26] S. Yves, R. Fleury, T. Berthelot, M. Fink, F. Lemoult, and G. Lerosey, Crystalline metamaterials for topological properties at subwavelength scales, Nat. Commun. **8**, 16023 (2017).

[27] M. S. Rudner and N. H. Lindner, Band structure engineering and non-equilibrium dynamics in Floquet topological insulators, Nat. Rev. Phys. **2**, 229 (2020).

[28] M. A. Bandres, M. Rechtsman, A. Szameit, and M. Segev, *CLEO: 2014* (Optica Publishing Group, Washington, 2014), p. FF2D.3.

[29] H. Zhong, R. Wang, F. Ye, J. Zhang, L. Zhang, Y. P. Zhang, M. R. Belić, and Y. Q. Zhang, Topological insulator properties of photonic kagome helical waveguide arrays, Results Phys. **12**, 996 (2019).

[30] M. A. Bandres, M. C. Rechtsman, and M. Segev, Topological Photonic Quasicrystals: Fractal Topological Spectrum and Protected Transport, Phys. Rev. X **6**, 011016 (2016).

[31] T. Biesenthal, L. J. Maczewsky, Z. Yang, M. Kremer, M. Segev, A. Szameit, and M. Heinrich, Fractal photonic topological insulators, Science **376**, 1114 (2022).

[32] L. J. Maczewsky, J. M. Zeuner, S. Nolte, and A. Szameit, Observation of photonic anomalous Floquet topological insulators, Nat. Commun. **8**, 13756 (2017).

[33] S. Mukherjee, A. Spracklen, M. Valiente, E. Andersson, P. Öhberg, N. Goldman, and R. R. Thomson, Experimental observation of anomalous topological edge modes in a slowly driven photonic lattice, Nat. Commun. **8**, 13918 (2017).

[34] W. Song, H. Li, S. Gao, C. Chen, S. Zhu, and T. Li, Subwavelength self-imaging in cascaded waveguide arrays, Adv. Photonics **2**, 036001 (2020).

[35] Y. Q. Zhang, Y. V. Kartashov, Y. P. Zhang, L. Torner, and D. V. Skryabin, Resonant edge-state switching in polariton topological insulators, Laser Photonics Rev. **12**, 1700348 (2018).

[36] H. Zhong, Y. V. Kartashov, Y. Q. Zhang, D. Song, Y. P. Zhang, F. Li, and Z. Chen, Rabi-like oscillation of photonic topological valley Hall edge states, Opt. Lett. **44**, 3342 (2019).

[37] Y. Q. Zhang, Y. V. Kartashov, Y. P. Zhang, L. Torner, and D. V. Skryabin, Inhibition of tunneling and edge state control

in polariton topological insulators, APL Photonics **3**, 120801 (2018).

[38] J. K. Asbóth, B. Tarasinski, and P. Delplace, Chiral symmetry and bulk-boundary correspondence in periodically driven one-dimensional systems, Phys. Rev. B **90**, 125143 (2014).

[39] V. Dal Lago, M. Atala, and L. E. F. Foa Torres, Floquet topological transitions in a driven one-dimensional topological insulator, Phys. Rev. A **92**, 023624 (2015).

[40] M. Fruchart, Complex classes of periodically driven topological lattice systems, Phys. Rev. B **93**, 115429 (2016).

[41] Y. Q. Zhang, Y. V. Kartashov, F. Li, Z. Y. Zhang, Y. P. Zhang, M. R. Belić, and M. Xiao, Edge states in dynamical superlattices, ACS Photonics **4**, 2250 (2017).

[42] J. Petráček and V. Kuzmiak, Dynamics and transport properties of Floquet topological edge modes in coupled photonic waveguides, Phys. Rev. A **101**, 033805 (2020).

[43] J. K. Asbóth, L. Oroszlány, and A. Pályi, The Su-Schrieffer-Heeger (SSH) model, in *A Short Course on Topological Insulators: Band Structure and Edge States in One and Two Dimensions* (Springer, Cham, 2016), pp. 1–22.

[44] Q. Cheng, Y. Pan, H. Wang, C. Zhang, D. Yu, A. Gover, H. Zhang, T. Li, L. Zhou, and S. Zhu, Observation of Anomalous π Modes in Photonic Floquet Engineering, Phys. Rev. Lett. **122**, 173901 (2019).

[45] S. Wu, W. Song, S. Gao, Y. Chen, S. Zhu, and T. Li, Floquet π mode engineering in non-Hermitian waveguide lattices, Phys. Rev. Res. **3**, 023211 (2021).

[46] W. Song, Y. Chen, H. Li, S. Gao, S. Wu, C. Chen, S. Zhu, and T. Li, Gauge-induced Floquet topological states in photonic waveguides, Laser Photonics Rev. **15**, 2000584 (2021).

[47] A. Sidorenko, Z. Fedorova, A. Abouelela, J. Kroha, and S. Linden, Real- and Fourier-space observation of the anomalous π mode in Floquet engineered plasmonic waveguide arrays, Phys. Rev. Res. **4**, 033184 (2022).

[48] Z. Cheng, R. W. Bomantara, H. Xue, W. Zhu, J. Gong, and B. Zhang, Observation of $\pi/2$ Modes in an Acoustic Floquet System, Phys. Rev. Lett. **129**, 254301 (2022).

[49] D. Smirnova, D. Leykam, Y. Chong, and Y. Kivshar, Nonlinear topological photonics, Appl. Phys. Rev. **7**, 021306 (2020).

[50] Y. V. Kartashov and D. V. Skryabin, Modulational instability and solitary waves in polariton topological insulators, Optica **3**, 1228 (2016).

[51] Y. V. Kartashov and D. V. Skryabin, Bistable Topological Insulator with Exciton-Polaritons, Phys. Rev. Lett. **119**, 253904 (2017).

[52] L. J. Maczewsky, M. Heinrich, M. Kremer, S. K. Ivanov, M. Ehrhardt, F. Martinez, Y. V. Kartashov, V. V. Konotop, L. Torner, D. Bauer, and A. Szameit, Nonlinearity-induced photonic topological insulator, Science **370**, 701 (2020).

[53] Y. Hadad, J. C. Soric, A. B. Khanikaev, and A. Alù, Self-induced topological protection in nonlinear circuit arrays, Nat. Electron. **1**, 178 (2018).

[54] F. Zangeneh-Nejad and R. Fleury, Nonlinear Second-Order Topological Insulators, Phys. Rev. Lett. **123**, 053902 (2019).

[55] Y. Lumer, Y. Plotnik, M. C. Rechtsman, and M. Segev, Self-Localized States in Photonic Topological Insulators, Phys. Rev. Lett. **111**, 243905 (2013).

[56] S. Mukherjee and M. C. Rechtsman, Observation of Floquet solitons in a topological bandgap, Science **368**, 856 (2020).

[57] D. Leykam and Y. D. Chong, Edge Solitons in Nonlinear-Photonic Topological Insulators, Phys. Rev. Lett. **117**, 143901 (2016).

[58] M. J. Ablowitz and J. T. Cole, Tight-binding methods for general longitudinally driven photonic lattices: Edge states and solitons, Phys. Rev. A **96**, 043868 (2017).

[59] S. K. Ivanov, Y. V. Kartashov, A. Szameit, L. Torner, and V. V. Konotop, Vector topological edge solitons in Floquet insulators, ACS Photonics **7**, 735 (2020).

[60] H. Zhong, S. Xia, Y. Zhang, Y. Li, D. Song, C. Liu, and Z. Chen, Nonlinear topological valley Hall edge states arising from type-II Dirac cones, Adv. Photonics **3**, 056001 (2021).

[61] M. S. Kirsch, Y. Zhang, M. Kremer, L. J. Maczewsky, S. K. Ivanov, Y. V. Kartashov, L. Torner, D. Bauer, A. Szameit, and M. Heinrich, Nonlinear second-order photonic topological insulators, Nat. Phys. **17**, 995 (2021).

[62] Z. Hu, D. Bongiovanni, D. Jukić, E. Jajtić, S. Xia, D. Song, J. Xu, R. Morandotti, H. Buljan, and Z. Chen, Nonlinear control of photonic higher-order topological bound states in the continuum, Light: Sci. Appl. **10**, 164 (2021).

[63] M. Jürgensen, S. Mukherjee, and M. C. Rechtsman, Quantized nonlinear Thouless pumping, Nature (London) **596**, 63 (2021).

[64] Q. Fu, P. Wang, Y. V. Kartashov, V. V. Konotop, and F. Ye, Nonlinear Thouless Pumping: Solitons and Transport Breakdown, Phys. Rev. Lett. **128**, 154101 (2022).

[65] Q. Fu, P. Wang, Y. V. Kartashov, V. V. Konotop, and F. Ye, Two-Dimensional Nonlinear Thouless Pumping of Matter Waves, Phys. Rev. Lett. **129**, 183901 (2022).

[66] R. Parker, A. Aceves, J. Cuevas-Maraver, and P. G. Kevrekidis, Floquet solitons in square lattices: Existence, stability, and dynamics, Phys. Rev. E **105**, 044211 (2022).

[67] Y. V. Kartashov, A. A. Arkhipova, S. A. Zhuravitskii, N. N. Skryabin, I. V. Dyakonov, A. A. Kalinkin, S. P. Kulik, V. O. Kompanets, S. V. Chekalin, L. Torner, and V. N. Zadkov, Observation of Edge Solitons in Topological Trimer Arrays, Phys. Rev. Lett. **128**, 093901 (2022).

[68] L. Li, W. Kong, and F. Chen, Femtosecond laser-inscribed optical waveguides in dielectric crystals: A concise review and recent advances, Adv. Photonics **4**, 024002 (2022).

[69] The refractive index profile in a 2D array can be written as $\mathcal{R}(x, y, z) = p \sum_m \sum_n e^{-(x_{1m}^2+y_{1n}^2)/d^2} + e^{-(x_{2m}^2+y_{1n}^2)/d^2} + e^{-(x_{1m}^2+y_{2n}^2)/d^2} + e^{-(x_{2m}^2+y_{2n}^2)/d^2}$, where $y_{1n} = y_n - a/4 - r\sin(\omega z)$ and $y_{2n} = y_n + a/4 + r\sin(\omega z)$, with $y_n = y + na$ and n being an integer.

[70] D. Leykam, M. C. Rechtsman, and Y. D. Chong, Anomalous Topological Phases and Unpaired Dirac Cones in Photonic Floquet Topological Insulators, Phys. Rev. Lett. **117**, 013902 (2016).

[71] S. K. Ivanov, Y. Q. Zhang, Y. V. Kartashov, and D. V. Skryabin, Floquet topological insulator laser, APL Photonics **4**, 126101 (2019).

[72] See Supplemental Material at http://link.aps.org/supplemental/10.1103/PhysRevA.107.L021502 for the method to calculate the quasispectrum and π-mode solitons, for the π-mode solitons in the presence of defects in the array, and for results at $r = 0.3$ where the quasienergy of the linear π-mode falls into the bulk band.

[73] B.-Y. Xie, G.-X. Su, H.-F. Wang, H. Su, X.-P. Shen, P. Zhan, M.-H. Lu, Z.-L. Wang, and Y.-F. Chen, Visualization of Higher-Order Topological Insulating Phases in Two-Dimensional

Dielectric Photonic Crystals, Phys. Rev. Lett. **122**, 233903 (2019).

[74] X.-D. Chen, W.-M. Deng, F.-L. Shi, F.-L. Zhao, M. Chen, and J.-W. Dong, Direct Observation of Corner States in Second-Order Topological Photonic Crystal Slabs, Phys. Rev. Lett. **122**, 233902 (2019).

[75] M. Kim and J. Rho, Topological edge and corner states in a two-dimensional photonic Su-Schrieffer-Heeger lattice, Nanophotonics **9**, 3227 (2020).

[76] Y. Peng and G. Refael, Floquet Second-Order Topological Insulators from Nonsymmorphic Space-Time Symmetries, Phys. Rev. Lett. **123**, 016806 (2019).

[77] H. Hu, B. Huang, E. Zhao, and W. V. Liu, Dynamical Singularities of Floquet Higher-Order Topological Insulators, Phys. Rev. Lett. **124**, 057001 (2020).

[78] B. Huang and W. V. Liu, Floquet Higher-Order Topological Insulators with Anomalous Dynamical Polarization, Phys. Rev. Lett. **124**, 216601 (2020).